

Phase relationships and structural, magnetic, and thermodynamic properties of alloys in the pseudobinary $\text{Er}_5\text{Si}_4\text{-Er}_5\text{Ge}_4$ system

A. O. Pecharsky,¹ K. A. Gschneidner, Jr.,^{1,2} V. K. Pecharsky,^{1,2,*} D. L. Schlage,¹ and T. A. Lograsso¹

¹*Materials and Engineering Physics Program, Ames Laboratory of the United States Department of Energy, Iowa State University, Ames, Iowa 50011-3020, USA*

²*Department of Materials Science and Engineering, Iowa State University, Ames, Iowa 50011-2300, USA*

(Received 29 April 2004; published 29 October 2004)

The room temperature crystal structures of $\text{Er}_5\text{Si}_x\text{Ge}_{4-x}$ alloys change systematically with the concentration of Ge from the orthorhombic Gd_5Si_4 -type when $x=4$, to the monoclinic $\text{Gd}_5\text{Si}_2\text{Ge}_2$ type when $3.5 \leq x \leq 3.9$ and to the orthorhombic Sm_5Ge_4 type for $x \leq 3$. The Curie-Weiss behavior of $\text{Er}_5\text{Si}_x\text{Ge}_{4-x}$ materials is consistent with the Er^{3+} state. The compounds order magnetically below 30 K, apparently adopting complex noncollinear magnetic structures with magnetization not reaching saturation in 50 kOe magnetic fields. In Er_5Si_4 , the structural-only transformation from the monoclinic $\text{Gd}_5\text{Si}_2\text{Ge}_2$ -type to the orthorhombic Gd_5Si_4 -type phase occurs around 218 K on heating. Intriguingly, the temperature of this polymorphic transformation is weakly dependent on magnetic fields as low as 40 kOe ($dT/dH = -0.058$ K/kOe) when the material is in the paramagnetic state nearly 200 K above its spontaneous magnetic ordering temperature. It appears that a magnetostructural transition may be induced in the 5:4 erbium silicide at ~ 18 K and above by 75 kOe and higher magnetic fields. Only Er_5Si_4 but none of the other studied $\text{Er}_5\text{Si}_x\text{Ge}_{4-x}$ alloys exhibit magnetic field induced transformations, which are quite common in the closely related $\text{Gd}_5\text{Si}_x\text{Ge}_{4-x}$ system. The magnetocaloric effects of the $\text{Er}_5\text{Si}_x\text{Ge}_{4-x}$ alloys are moderate.

DOI: 10.1103/PhysRevB.70.144419

PACS number(s): 75.20.En, 74.62.Bf, 74.62.Yb, 75.30.Sg

INTRODUCTION

Both the existence and crystallographic data of binary rare earth-germanium and rare earth-silicon compounds with the R_5T_4 stoichiometries (R=rare earth element, T=Si or Ge) were originally reported by Smith *et al.*¹ Soon after, Holtzberg *et al.*² described phase relationships in the pseudobinary $\text{Gd}_5\text{Si}_4\text{-Gd}_5\text{Ge}_4$ system. They² also confirmed the crystallography and provided magnetic property data for the binary R_5T_4 silicides and germanides of heavy lanthanides, i.e., for R=Gd, Tb, Dy, Ho, and Er. All silicides were classified as ferromagnets. Within the series, Gd_5Si_4 has the highest Curie temperature, $T_C = \sim 340$ K, and ferromagnetic ordering temperatures gradually decrease from $T_C = 225$ K for Tb_5Si_4 , to $T_C = 140$ K, 76 K, and 25 K for Dy_5Si_4 , Ho_5Si_4 , and Er_5Si_4 , respectively. Conversely, the germanides were reported to order antiferromagnetically at 15 and 47 K for Gd_5Ge_4 (recent data,³⁻⁹ however, indicate that Néel temperature of Gd_5Ge_4 is ~ 128 K), 30 K for Tb_5Ge_4 , 40 K for Dy_5Ge_4 , 21 K for Ho_5Ge_4 , and 7 K for Er_5Ge_4 . In the $\text{Gd}_5\text{Si}_x\text{Ge}_{4-x}$ system, Holtzberg *et al.*² also found two extended solid solutions based on both Gd_5Si_4 and Gd_5Ge_4 , and a new ternary phase with an unknown crystal structure.

The discovery of the giant magnetocaloric effect in $\text{Gd}_5\text{Si}_2\text{Ge}_2$ (Ref. 10) triggered a widespread research of the pseudobinary $\text{Gd}_5\text{Si}_x\text{Ge}_{4-x}$ system. In 1997, Pecharsky and Gschneidner¹¹ reported, and later Morellon *et al.*¹² and Pecharsky *et al.*¹³ refined the pseudobinary phase diagram. At present, it is well established that the Si-rich alloys adopt the orthorhombic Gd_5Si_4 -type structure at room temperature when $x \geq 2.1$ and that they order ferromagnetically on cooling *via* a second-order phase transition. The intermediate solid solution alloys with $1.5 \leq x < 2.1$ crystallize in the

monoclinic $\text{Gd}_5\text{Si}_2\text{Ge}_2$ -type structure at room temperature. When cooled, they undergo a transformation to the Gd_5Si_4 -type structure, which is coupled with ferromagnetic ordering. Thermodynamically, these are first-order phase transitions. The Ge-rich solid solution alloys have the orthorhombic Sm_5Ge_4 -type crystal structure at room temperature when $x \leq 1.2$ and the majority of them exhibit two successive transformations below room temperature. A second-order paramagnetic to antiferromagnetic transition occurs at nearly constant temperature (~ 130 K) regardless of the alloy composition. A first-order transformation, during which a crystallographic transition from the Sm_5Ge_4 - to Gd_5Si_4 -type structure is coupled with an antiferromagnetic to ferromagnetic transition, is observed at lower temperatures with T_C strongly dependent on the value of x . It is worth noting that in a zero magnetic field, only the high temperature paramagnetic-antiferromagnetic transition occurs in pure Gd_5Ge_4 .³⁻⁹ Both the monoclinic $\text{Gd}_5\text{Si}_2\text{Ge}_2$ - and the orthorhombic Sm_5Ge_4 -type alloys exhibit the giant magnetocaloric effect around their respective first-order magnetostructural phase transition temperatures.¹⁴

Of the eight possible $\text{R}_5\text{Si}_x\text{Ge}_{4-x}$ systems, where R is heavy lanthanide, the $\text{Gd}_5\text{Si}_x\text{Ge}_{4-x}$ alloys are the most studied to date. Over the last few years, several reports describing both the interaction of components and physical properties of compounds have been published for $\text{Tb}_5\text{Si}_x\text{Ge}_{4-x}$ by Morellon *et al.*,^{15,16} Huang *et al.*,¹⁷ Ritter *et al.*,¹⁸ Tegus *et al.*,¹⁹ Thuy *et al.*,^{20,21} Yoa *et al.*,²² and Lee *et al.*,²³ and for $\text{Dy}_5\text{Si}_x\text{Ge}_{4-x}$ by Gschneidner *et al.*²⁴ and Ivchenko *et al.*²⁵ Preliminary results have been also reported about some individual intermetallics, including $\text{Ho}_5\text{Si}_2\text{Ge}_2$ by Thuy *et al.*,²⁶ Yb_5Si_4 by Cerny and Alamdi-Yardi,²⁷ and Yb_5Ge_4 by Pani and Palenzona.²⁸ Despite limited amount of available data, it

is quite evident that systems with heavy lanthanides demonstrate both similarities and differences when compared to the $\text{Gd}_5\text{Si}_x\text{Ge}_{4-x}$ alloys, thus pointing to a complexity of interactions between heavy lanthanides, germanium, and silicon at the R_5T_4 stoichiometries.

Only a little research has been carried out on the $\text{Er}_5\text{Si}_x\text{Ge}_{4-x}$ system. Besides original reports by Smith *et al.*¹ and Holtzberg *et al.*,² phase equilibria, electrical resistivity, and thermal expansion of binary silicides of Er were reported by Luzan *et al.*²⁹ but only above room temperature. According to Ref. 29, Er_5Si_4 forms peritectically at 2150 K and it belongs to the Sm_5Ge_4 -type structure with lattice parameters $a=7.28$, $b=14.37$, and $c=7.595$ Å at room temperature. On the contrary, Kotur and Parasyuk³⁰ claim that they did not observe the formation of Er_5Si_4 at 870 K. Recently, Pecharsky *et al.*³¹ and Mozharivskiy *et al.*³² established that Er_5Si_4 adopts the Gd_5Si_4 -type structure at room temperature. On cooling, it transforms into the monoclinic $\text{Gd}_5\text{Si}_2\text{Ge}_2$ -type phase between 210 and 200 K while remaining paramagnetic, and the monoclinic polymorph of Er_5Si_4 orders magnetically at ~ 30 K. Its magnetic ground state is complex showing a distinct ferromagnetic component.³¹ According to our preliminary temperature dependent x-ray powder diffraction studies,³³ the magnetically ordered Er_5Si_4 retains the monoclinic $\text{Gd}_5\text{Si}_2\text{Ge}_2$ -type structure down to ~ 5 K in a zero magnetic field. In this respect, the silicide of erbium is quite different from all other members of the extended $\text{R}_5\text{Si}_x\text{Ge}_{4-x}$ family studied to date, where the ferromagnetic order has been always associated with the Gd_5Si_4 -type structure.

Here we report on the relationships between chemical composition, crystal structure, magnetic, thermal, and magnetocaloric properties of several pseudobinary alloys in the $\text{Er}_5\text{Si}_x\text{Ge}_{4-x}$ system. As we will describe below, this system exhibits much greater deviations from the related $\text{Gd}_5\text{Si}_x\text{Ge}_{4-x}$ alloys^{11–13} when compared to $\text{Tb}_5\text{Si}_x\text{Ge}_{4-x}$ ^{15–22} and $\text{Dy}_5\text{Si}_x\text{Ge}_{4-x}$,^{24,25} thus demonstrating that physical properties of these intriguing R_5T_4 family of materials can be adjusted over a broad range of values.

ALLOY PREPARATION AND CHARACTERIZATION

A total of 13 alloys in the $\text{Er}_5\text{Si}_x\text{Ge}_{4-x}$ system with x varying from ~ 4 to 0 were prepared by arc melting of stoichiometric mixtures of pure components in an argon atmosphere on a water-cooled copper hearth using high purity components. The Er metal was prepared by the Materials Preparation Center of the Ames Laboratory and it was 99.86 at. % (99.99 wt. %) pure. The major impurities in ppm atomic (and in ppm by weight) were as follows: O, 400 (40); C, 280 (20); N, 70 (6); F, 120 (14); H, 170 (1), and Fe, 30 (10). The Si and Ge were purchased from Meldform Metals (United Kingdom) and were 99.999 wt. % pure. Every alloy was remelted six times; alloy buttons were turned over after each melting to improve their homogeneity. The weight of each alloy did not exceed 20 g to ensure fast cooling. Weight losses after the melting were in the range from 0.3 to 0.5 wt. %, therefore alloy stoichiometries were assumed to remain unchanged after the preparation. All the

alloys were examined in the as-prepared condition, without heat treatment.

In addition to arc-melted buttons, in this study we examined nonoriented large-grain leftovers extracted from a sample of Er_5Si_4 which has been used to prepare single crystals by Bridgman technique. This alloy was first arc melted (both the Er and Si were of the same purity as mentioned above) and then electron beam welded in a tungsten Bridgman crucible. The crucible was placed inside a tungsten mesh resistance furnace under a pressure of 6.7×10^{-4} Pa and slowly heated to 1970 K. Then the chamber was back-filled with high purity argon to 2.8×10^5 Pa to equalize the pressures inside and outside the crucible. The crucible was then heated to 2320 K, after which it was withdrawn from the heat zone at the rate of 8 mm/h. While some reaction of the melt with the crucible walls was noted, x-ray powder diffraction indicated phase purity of the as-grown ingot. The samples described in this work were extracted from the middle of the as-solidified ingot as scraps that remained after cutting out specimens for other property measurements.

The crystal structures and phase compositions of the alloys were characterized by x-ray powder diffraction. The x-ray powder diffraction data were collected on a Rigaku TTRAX rotating anode diffractometer equipped with a wide angle goniometer using $\text{Mo } K\alpha$ radiation between 8° – 11° and 50° of 2θ with a 0.01° step. The crystal structures were refined in an isotropic approximation by using Rietveld technique.³⁴ The resulting profile residuals (R_p) were lower than 10% and the derived Bragg residuals (R_B) did not exceed 6%.

Magnetic susceptibility and magnetization measurements were performed on a Lake Shore dc/ac magnetometer-susceptometer, model 7225. Temperature dependent magnetic susceptibilities were measured between 5 and 320 K in an ac magnetic field with a 5 Oe amplitude and a 125 Hz frequency in a zero bias dc field. Magnetization was measured as a function of temperature between 5 and 320 K in various dc magnetic fields between 1 and 50 kOe. Isothermal magnetization data were collected in the vicinities of magnetic phase transition temperatures in dc magnetic fields varying from 0 to 50 kOe with a 2 kOe step.

The heat capacities were measured using a semiadiabatic heat pulse calorimeter³⁵ from ~ 3.5 to 350 K in various constant dc magnetic fields ranging from 0 to 100 kOe. The phase transition temperatures were determined from both the magnetic and calorimetric measurements. The magnetocaloric effect in terms of the isothermal magnetic entropy change (ΔS_M) and the adiabatic temperature change (ΔT_{ad}) was calculated from either or both magnetic and calorimetric data as described by Pecharsky and Gschneidner.^{36,37}

EXPERIMENTAL RESULTS AND DISCUSSION

Erbium silicide: Er_5Si_4

The room-temperature crystal structure of Er_5Si_4 was confirmed using x-ray powder diffraction data collected from several different samples at ambient temperature and employing the crystallographic parameters obtained from the single crystal structural investigation in Ref. 31. The refined

TABLE I. Room temperature crystallographic data of selected compounds in the Er_5Si_4 - Er_5Ge_4 pseudobinary system.

Composition	Structure type	Space group	Unit cell dimensions			γ , °	Reference
			a , Å	b , Å	c , Å		
Er_5Si_4	Sm_5Ge_4	$Pnma$	7.27	14.32	7.58		1
Er_5Si_4	Sm_5Ge_4	$Pnma$	7.289	14.371	7.591		2
Er_5Si_4	Sm_5Ge_4	$Pnma$	7.28	14.37	7.595		29
Er_5Si_4 (I) ^a	Gd_5Si_4	$Pnma$	7.2838(6)	14.363(1)	7.5943(6)		31
Er_5Si_4 ^{b,c} (I) ^a	Gd_5Si_4	$Pnma$	7.2931(3)	14.374(1)	7.5980(3)		d
$\text{Er}_{5.05}\text{Si}_4$ ^{b,c} (II) ^a	Gd_5Si_4	$Pnma$	7.2927(3)	14.374(1)	7.5973(3)		d
Er_5Si_4 ^c (III) ^a	Gd_5Si_4	$Pnma$	7.2940(6)	14.374(1)	7.5973(5)		d
$\text{Er}_5\text{Si}_{3.8}\text{Ge}_{0.2}$	$\text{Gd}_5\text{Si}_2\text{Ge}_2$	$P112_1/a$	7.3681(3)	14.412(1)	7.5728(4)	92.958(3)	d
$\text{Er}_5\text{Si}_{3.6}\text{Ge}_{0.4}$	$\text{Gd}_5\text{Si}_2\text{Ge}_2$	$P112_1/a$	7.3745(4)	14.412(1)	7.5746(4)	92.960(3)	d
$\text{Er}_5\text{Si}_{3.5}\text{Ge}_{0.5}$	$\text{Gd}_5\text{Si}_2\text{Ge}_2$	$P112_1/a$	7.3777(3)	14.420(1)	7.5786(3)	92.948(2)	d
$\text{Er}_5\text{Si}_3\text{Ge}$	Sm_5Ge_4	$Pnma$	7.4528(3)	14.443(1)	7.5456(3)		d
$\text{Er}_5\text{Si}_{2.9}\text{Ge}_{1.1}$	Sm_5Ge_4	$Pnma$	7.4548(3)	14.442(1)	7.5456(3)		d
$\text{Er}_5\text{Si}_{2.5}\text{Ge}_{1.5}$	Sm_5Ge_4	$Pnma$	7.4671(3)	14.451(1)	7.5517(3)		d
$\text{Er}_5\text{Si}_{1.95}\text{Ge}_{2.05}$	Sm_5Ge_4	$Pnma$	7.4862(3)	14.466(1)	7.5609(3)		d
Er_5Ge_4	Sm_5Ge_4	$Pnma$	7.5448(3)	14.515(1)	7.6081(3)		d
Er_5Ge_4	Sm_5Ge_4	$Pnma$	7.51	14.41	7.59		1
Er_5Ge_4	Sm_5Ge_4	$Pnma$	7.536	14.506	7.600		2

^aSample I is the stoichiometric arc-melted alloy containing ~ 5 vol. % of ErSi_{1-x} impurity; sample II is off-stoichiometric arc-melted alloy, which is a single phase material within the sensitivity of x-ray powder diffraction analysis; sample III is the stoichiometric Bridgman-grown single phase material.

^bDiffraction data were collected at $T=300$ K.

^cDuring Rietveld refinement, a small yet measurable amount of the monoclinic polymorph of Er_5Si_4 was also detected (Ref. 33), but these results are not included in the table, nor are they shown in Fig. 1.

^dThis study.

lattice parameters of Er_5Si_4 are listed in Table I together with those reported previously in the literature and all of the other $\text{Er}_5\text{Si}_x\text{Ge}_{4-x}$ alloys examined in the course of this study. The results of Rietveld refinement for Er_5Si_4 are in agreement with our single crystal study,³¹ confirming that the 5:4 erbium silicide belongs to the Gd_5Si_4 -type crystal structure and not to the Sm_5Ge_4 type as was assumed earlier^{1,2,29} (the difference between the Sm_5Ge_4 - and Gd_5Si_4 -type structures has been described by Pecharsky and Gschneidner^{11,38} and by Choe *et al.*³⁹).

The x-ray powder diffraction pattern [Fig. 1(a)] of the *arc-melted stoichiometric* Er_5Si_4 , hereafter called sample I, clearly indicates the presence of a small amount of an impurity phase. The latter was identified as erbium monosilicide, ErSi . The concentration of the latter in the as-prepared Er_5Si_4 alloy is 5 ± 1 vol. % as determined in the course of Rietveld refinement. Therefore, we prepared an *off-stoichiometric alloy*, $\text{Er}_{5.05}\text{Si}_4$, henceforth referred to as sample II, in an attempt to obtain a single-phase material. As seen in Fig. 1(b), no impurity phase(s) can be detected in this alloy within the sensitivity of the x-ray powder diffraction technique. The unit cell dimensions of $\text{Er}_{5.05}\text{Si}_4$ (Table I) show no statistically significant differences when compared to those of Er_5Si_4 . Considering the full occupancy of all sites,³¹ we conclude that Er_5Si_4 is a stoichiometric compound, and despite small weight losses observed during the arc melting, the

evaporation of the Er metal was substantial enough to shift the as-prepared Er_5Si_4 alloy into the $\text{ErSi}_{1-x} + \text{Er}_5\text{Si}_4$ two-phase region of the Er-Si phase diagram.²⁹ Consistent with this conclusion, is the x-ray powder diffraction pattern (not shown) of the *stoichiometric* Er_5Si_4 prepared using the *Bridgman technique*, from now on called sample III, indicating a single phase alloy because evaporative losses from a sealed crucible were indeed negligible. Its unit cell dimensions (Table I) deviate from those of both arc-melted materials by no more than two standard deviations, i.e., the differences in the unit cell dimensions of the three different Er_5Si_4 samples, are statistically insignificant. A non-negligible discrepancy seen between the three sets of powder diffraction data (samples I, II, and III) and the unit cell dimensions determined in the course of single crystal (sample I) investigation³¹ is likely related to a lower absolute precision attainable in a single crystal diffraction experiment when compared with the high resolution powder diffraction data.

For the arc-melted alloy, the dc magnetization data (Figs. 2 and 3) indicate two phase transformations that occur in Er_5Si_4 below room temperature. On cooling, a structural transition^{31,32} is observed in the paramagnetic state between 210 K to 200 K (Fig. 3, inset) and a ferromagneticlike or ferrimagneticlike ordering occurs in low magnetic fields at ~ 30 K (Figs. 2 and 3). The structural transition is hysteretic:

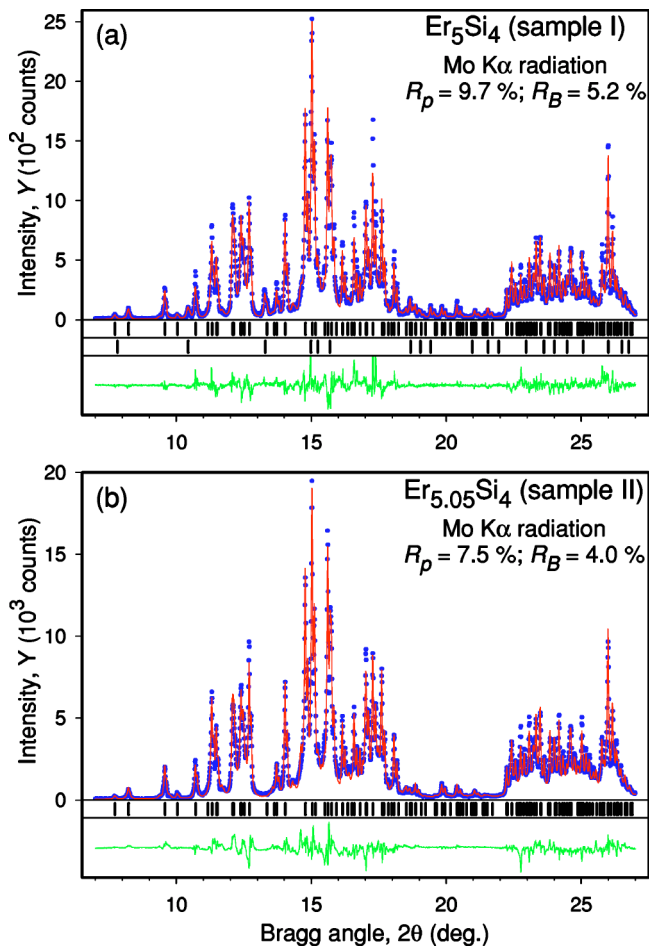


FIG. 1. (Color online) Fragments of the x-ray powder diffraction patterns of (a) the arc-melted Er_5Si_4 alloy (sample I) and (b) the arc-melted $\text{Er}_{5.05}\text{Si}_4$ alloy (sample II). The points represent observed data and the lines drawn through the data points correspond to the calculated patterns. The differences, $Y_{\text{obs}} - Y_{\text{calc}}$, are shown at the bottom of each plot. The upper set of vertical bars in (a) and the only set in (b) represent calculated positions of Bragg peaks ($K\alpha_1$ components only) of the orthorhombic Er_5Si_4 . The lower set of vertical bars in (a) indicates the same for ErSi , which belongs to the orthorhombic CrB-type structure. The most obvious difference between the two patterns is the absence in (b) of Bragg peaks at $2\theta = 10.44^\circ$ and 13.29° corresponding to ErSi impurity.

it takes place between 215 K and 225 K on heating, as illustrated in Fig. 3, inset. The behavior of the ac magnetic susceptibility (Fig. 2, inset) confirms the ferrimagneticlike nature of the low temperature magnetically ordered Er_5Si_4 phase and is consistent with gradually increasing coercivity below the Curie temperature. A small amount of the antiferromagnetic ErSi ($T_N = 11.5$ K,⁴⁰ as indicated by a vertical arrow in the inset in Fig. 2) present in the arc-melted Er_5Si_4 may contribute to a broad anomaly of χ'_{ac} , although as described below (see Fig. 4), the anomaly itself appears to be intrinsic to Er_5Si_4 .

The isothermal magnetization at 5 K (Fig. 3) remains far from saturation in a 50 kOe magnetic field, reaching only $\sim 65\%$ of the theoretically expected value assuming that the ordered magnetic moment of Er is $\mu = gJ = 9\mu_B$. The steplike

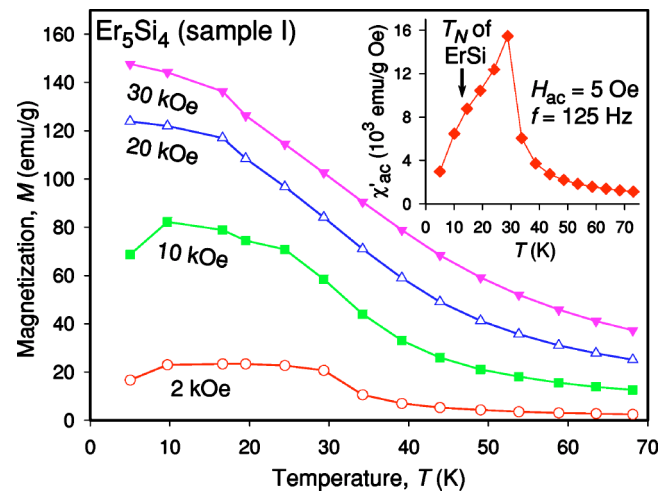


FIG. 2. (Color online) The dc magnetization of the arc melted polycrystalline Er_5Si_4 alloy (sample I) measured as a function of temperature in 2, 10, 20, and 30 kOe magnetic fields on heating the zero magnetic field cooled sample. The inset shows the behavior of the ac magnetic susceptibility of polycrystalline Er_5Si_4 . The short vertical arrow in the inset indicates Néel temperature of ErSi , which according to Ref. 40 is $T_N = 11.5$ K.

increase observed in the M vs H curve between 10 and 11 kOe is too large to be ascribed exclusively to the ErSi impurity [which is metamagnetic above 16 kOe at $T = 2.16$ K (Ref. 41)], and it is indicative of a magnetic field induced metamagnetic transition intrinsic to Er_5Si_4 . Although the low temperature magnetic structure of Er_5Si_4 remains unknown,^{42–44} available magnetic property data point to a complex noncollinear arrangement of the magnetic moments of Er below 30 K in low magnetic fields.

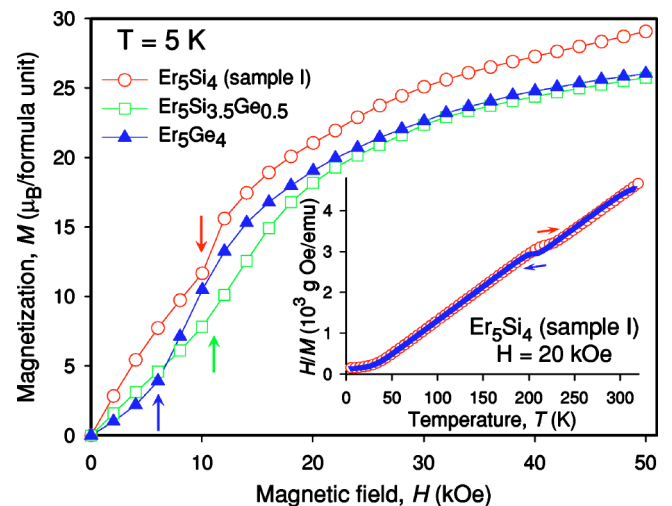


FIG. 3. (Color online) The dc magnetizations of the arc-melted polycrystalline Er_5Si_4 (sample I), $\text{Er}_5\text{Si}_{3.5}\text{Ge}_{0.5}$ and Er_5Ge_4 alloys as functions of magnetic field measured at $T = 5$ K. The vertical arrows point to the onsets of the corresponding metamagnetic transitions. The inverse magnetic susceptibility of polycrystalline Er_5Si_4 measured in a 20 kOe magnetic field during both cooling and heating is shown in the inset with the arrows indicating the direction of temperature change.

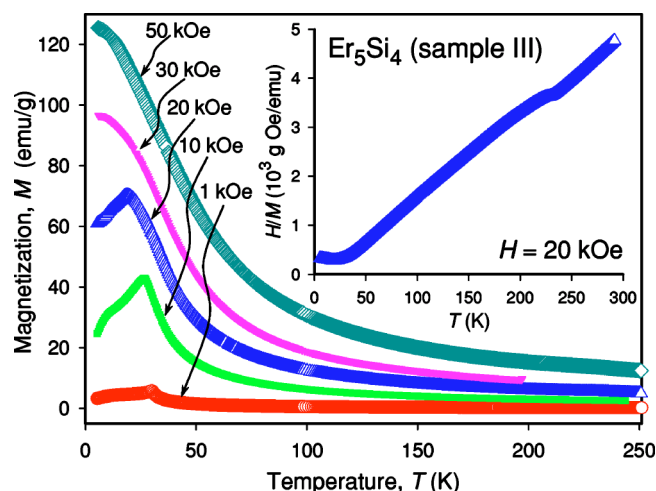


FIG. 4. (Color online) The dc magnetization of the nonoriented large-grain Er_5Si_4 (sample III) measured as a function of temperature in 1, 10, 20, 30, and 50 kOe magnetic fields during heating the zero magnetic field cooled specimen. The inset illustrates the H/M behavior measured on heating in a 20 kOe magnetic field.

For the single phase Er_5Si_4 (sample III), the magnetization versus temperature is shown in Fig. 4. It was measured using a randomly oriented apparently single-grain specimen⁴⁵ extracted from the material prepared using Bridgman technique in order to clarify whether or not the lowest temperature anomaly is intrinsic to Er_5Si_4 . By comparing both Fig. 2 and its inset with Fig. 4, it is easy to see that the lowest temperature anomaly around $T=12$ K is still present in the low field dc magnetization of pure Er_5Si_4 . In fact, it becomes much more pronounced when compared to the sample shown in Fig. 2. The anomaly is, therefore, intrinsic to Er_5Si_4 and its correspondence with the Néel temperature of ErSi is coincidental.

Even though the orientation of crystallographic axes of this specimen with respect to the magnetic field vector is unknown, the data presented in Fig. 4 shed some light on the

nature of the magnetic ordering at $T=30$ K and point to a considerable magnetocrystalline anisotropy of the compound (e.g., the values of magnetization in Fig. 4 are substantially lower than the corresponding values in Fig. 2). The temperature of the cusp, which is observed around 30 K in the 1 kOe $M(T)$ data, is suppressed to $T=27$ K and $T=19$ K by 10 and 20 kOe magnetic fields, respectively. This behavior is consistent with a strong antiferromagnetic component in the magnetic structure of the material. It is interesting to note that the temperature of the broad anomaly observed at ~ 12 K remains unaffected by magnetic fields of 20 kOe and below. In magnetic fields higher than 30 kOe, the $M(T)$ of Er_5Si_4 becomes consistent with the predominantly ferromagnetic or ferrimagnetic arrangement of spins in the material.

The magnetic ordering temperatures and the Curie-Weiss parameters of Er_5Si_4 are listed in Table II. Predictably, the structural change around 220 K has a significant effect on the paramagnetic Curie temperature of the material. The monoclinic polymorph of the 5:4 erbium silicide has lower paramagnetic Curie temperature ($\Theta_p=19.6$ K) when compared to the orthorhombic polymorph ($\Theta_p=30.3$ K). The lowering of Θ_p indicates a weakening of exchange interactions and is consistent with the notion that the presence of covalentlike Si_2 dimers results in strengthening of magnetic interactions between the two-dimensional slabs.^{38,46} The dimers are found between every slab in the Gd_5Si_4 type (the orthorhombic polymorph) and only between every other slab in the $\text{Gd}_5\text{Si}_2\text{Ge}_2$ type (the monoclinic phase).^{11,39} For both crystallographic modifications of the compound, positive paramagnetic Curie temperatures are indicative of the ferromagnetic or ferrimagnetic ground state of the material.

Consistent with the behavior of the magnetization, the heat capacity of the arc-melted Er_5Si_4 [sample I, Fig. 5(a)] also displays two distinct irregularities. The low-temperature λ -type anomaly, which occurs at ~ 30 K in zero magnetic field, is transformed into a rounded peak by increasing magnetic field as expected for a second-order paramagnetic-ferromagnetic (or ferrimagnetic) phase transformation. The high temperature peak observed between ~ 210 K and

TABLE II. Magnetic properties of selected compounds from the Er_5Si_4 - Er_5Ge_4 pseudobinary system.

Compound	Structure type	T_C or T_N (K)			Θ_p (K)	μ_{eff} (μ_B) ^a	Reference
		From $M(T)$	From $C_p(T)$				
Er_5Si_4	" Sm_5Ge_4 "	25		20	9.86	2	
Er_5Si_4 (I)	Gd_5Si_4			30.3 ^b	9.71 ^b	This study	
Er_5Si_4 (I)	$\text{Gd}_5\text{Si}_2\text{Ge}_2$ ^c	29	30	19.6 ^d	9.63 ^d	This study	
$\text{Er}_5\text{Si}_{3.5}\text{Ge}_{0.5}$	$\text{Gd}_5\text{Si}_2\text{Ge}_2$	25	28	15.9	9.55	This study	
$\text{Er}_5\text{Si}_3\text{Ge}$	Sm_5Ge_4	20	17	5.3	9.57	This study	
$\text{Er}_5\text{Si}_{2.5}\text{Ge}_{1.5}$	Sm_5Ge_4	18		12.3	9.39	This study	
$\text{Er}_5\text{Si}_{1.95}\text{Ge}_{2.05}$	Sm_5Ge_4	17	17	13.9	9.56	This study	
Er_5Ge_4	Sm_5Ge_4	14	14, 7.5	14.8	9.56	This study	
Er_5Ge_4	Sm_5Ge_4	7		10	9.73	2	

^aThe theoretical value of the effective magnetic moment for a free Er^{3+} ion is $9.58\mu_B$.

^bDetermined from the Curie-Weiss fit of the data measured on heating between 250 K and 310 K.

^cThe compound adopts this monoclinic crystal structure upon cooling below ~ 200 K.

^dDetermined from the Curie-Weiss fit of the data measured on heating between 50 and 190 K.

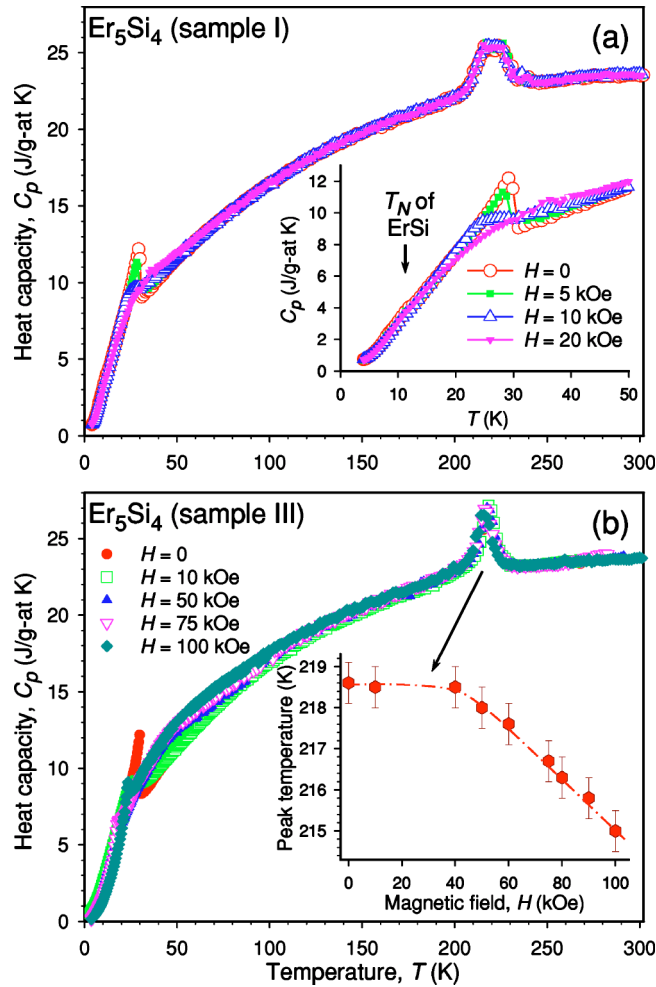


FIG. 5. (Color online) The heat capacities of (a) arc-melted Er_5Si_4 (sample I) and (b) large-grain Er_5Si_4 (sample III) measured from ~ 3.5 to 300 K in various magnetic fields after zero-field cooling the samples to ~ 3.5 K. The inset in (a) clarifies the behavior below 50 K, the inset in (b) shows the magnetic field dependence of the peak corresponding to the structural transformation (also see the inset of Fig. 6).

~ 240 K is magnetic field independent in this range of magnetic fields, and is indicative of a first-order transformation despite the ~ 40 K peak width. Both the behavior and location of this anomaly are commensurate with the structural transition observed in Er_5Si_4 in this temperature range.³¹ A minor broad abnormality observed around 11 K in the zero field heat capacity is in line with the ac magnetic susceptibility data and it may be slightly enhanced by the presence of ErSi impurity.

For the single phase large-grain Er_5Si_4 (sample III), the heat capacity [Fig. 5(b)] is in excellent agreement with all the results that have been already described above, except that the anomaly at ~ 218 K corresponding to the structural transformation narrows and clearly becomes a single peak instead of a double peak structure seen in Fig. 5(a). After subtracting the baseline heat capacity between 190 K and 240 K determined by a third order polynomial approximation of the data from 150 K to 190 K and from 240 K to 250 K and corresponding integration, the entropy

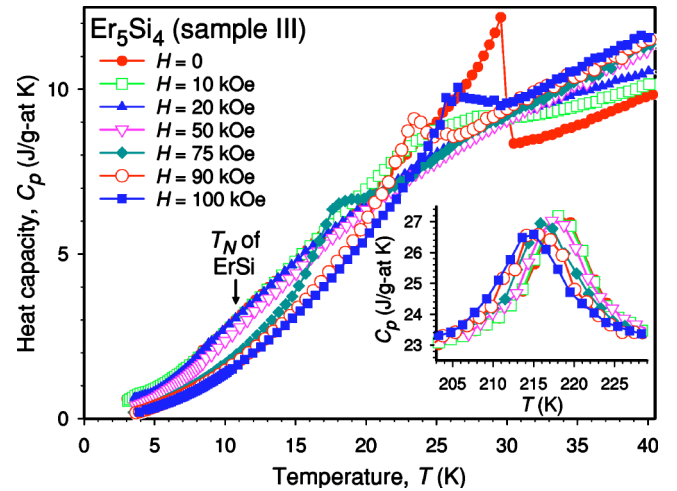


FIG. 6. (Color online) The low temperature heat capacity of large-grain Er_5Si_4 (sample III) measured in various magnetic fields after zero-field cooling the sample to ~ 3.5 K. The inset clarifies the behavior of the peak around 218 K.

of the polymorphic transformation of Er_5Si_4 is $\Delta S_{\text{tr}} = 0.24$ J/g at K.

Another unexpected feature is that the position of the 218 K heat capacity peak corresponding to the structural transition in the paramagnetic state is evidently influenced by magnetic field, as seen in the insets of Fig. 5(b) and Fig. 6. Both the peak and the underlying crystallographic-only transformation are suppressed nearly linearly between 40 and 100 kOe at the rate $dT/dH = -0.058$ K/kOe. To the best of our knowledge, to date there have been no reports that the relatively weak (40 to 100 kOe) magnetic field is able to measurably affect the temperature of a crystallographic transition in the paramagnetic state approximately 200 K above the spontaneous magnetic ordering temperature. Although we do not have sufficient data to speculate on the mechanism of this phenomenon, we believe that it is related to both the large localized magnetic moment of Er and presumably unusually strong spin-orbit coupling in the material. We also believe that the effect of the magnetic field on this polymorphic transformation that does not involve magnetic order should be highly anisotropic because we did not observe a measurable change in the position of the heat capacity peak in the polycrystalline Er_5Si_4 (samples I and II) in magnetic fields as high as 75 kOe (see Ref. 31 and Fig. 5).

The behavior of the heat capacity in the vicinities of both the low temperature and the high temperature anomalous regions is clarified in Fig. 6. Consistently with the magnetization data, a broad bump around 11.5 K remains field independent as long as the magnetic field is 50 kOe or lower. When the field reaches 75 kOe and greater, however, it induces an additional heat capacity peak suggestive of a metamagnetic transition, which rapidly and nearly linearly ($dT/dH = 0.32$ K/kOe) moves towards high temperature as the magnetic field increases. Thus, this new peak occurs at ~ 18 , ~ 23 , and ~ 26 K in the 75, 90, and 100 kOe magnetic fields, respectively. Both the appearance and the behavior of this peak resemble closely that observed in polycrystalline Gd_5Ge_4 (Ref. 8) except for the difference in the critical mag-

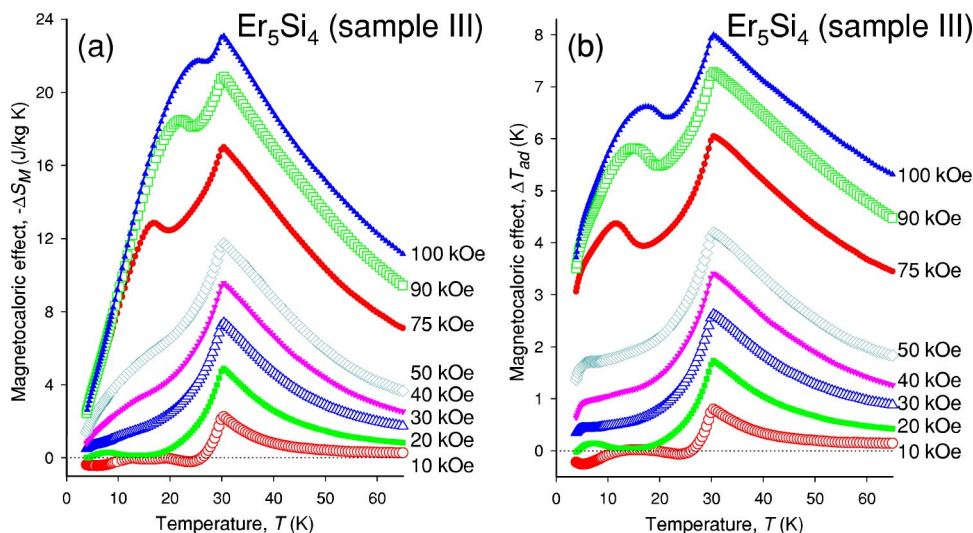


FIG. 7. (Color online) The magnetocaloric effect of Er_5Si_4 (sample III) calculated from heat capacity data: the isothermal magnetic entropy change (a) and the adiabatic temperature change (b). The values shown near the curves indicate the final magnetic field. The initial magnetic field was 0 in all cases.

netic fields: the field-induced heat capacity anomaly appears at 20 kOe in Gd_5Ge_4 , while it only becomes apparent at 75 kOe in Er_5Si_4 . It is quite feasible, therefore, that this behavior is reflective of a previously unknown magnetostructural transition that occurs in Er_5Si_4 in this range of temperatures and magnetic fields.

The magnetocaloric effect of Er_5Si_4 , calculated in terms of both the extensive (the isothermal magnetic entropy change, ΔS_M) and intensive (the adiabatic temperature change, ΔT_{ad}) variables from the heat capacity data, is shown in Fig. 7. At and above ~ 30 K, the MCE remains positive even for the lowest magnetic field change of 0 to 10 kOe, thus supporting a notion about the presence of a ferromagnetic signature in the ground state of Er_5Si_4 . The small negative MCE observed below ~ 30 K in a 10 kOe field is indicative of a complex magnetic structure. As the upper magnetic field increases from 10 to 100 kOe, the main MCE peak remains at $T=30.4$ K, which is consistent with a second order ferromagnetic ordering in a zero magnetic field and this peak represents a conventional contribution to the magnetocaloric effect. When the magnetic field reaches and exceeds 75 kOe, the new ΔS_M peaks are induced at 16.7, 22.1, and 25.7 K, and the new ΔT_{ad} peaks occur at 11.8, 15.0, and 17.5 K in 75, 90, and 100 kOe magnetic fields, respectively. The magnitudes of these additional peaks increase with the increasing field faster than the magnitudes of the main MCE peaks, which is similar to the behavior of the magnetocaloric effect in Gd_5Ge_4 ,⁴⁷ where a first order magnetostructural transition is induced by a magnetic field at low temperatures. Without additional crystallographic data, we can only speculate that since below ~ 200 K Er_5Si_4 adopts the monoclinic $\text{Gd}_5\text{Si}_2\text{Ge}_2$ -type crystal structure in both the paramagnetic and magnetically ordered states, the high magnetic fields (greater or equal to 75 kOe) induce a transition to the Gd_5Si_4 -type structure, which is coupled to the ferromagnetism of the material, just as it happens in Ge-rich $\text{Gd}_5\text{Si}_x\text{Ge}_{4-x}$ alloys.^{6,12}

Intermediate phase: $\text{Er}_5\text{Si}_{3.9}\text{Ge}_{0.1}$ to $\text{Er}_5\text{Si}_{3.5}\text{Ge}_{0.5}$

Upon substituting as little as 2.5 at. % of Ge for Si, the room temperature crystal structures of the $\text{Er}_5\text{Si}_x\text{Ge}_{4-x}$ alloys

change from the orthorhombic Gd_5Si_4 type to the monoclinic $\text{Gd}_5\text{Si}_2\text{Ge}_2$ type. The monoclinic structure is preserved at room temperature from the $\text{Er}_5\text{Si}_{3.9}\text{Ge}_{0.1}$ to $\text{Er}_5\text{Si}_{3.5}\text{Ge}_{0.5}$ stoichiometry, and an x-ray powder diffraction pattern of the latter composition is depicted in Fig. 8. The lattice parameters of several alloys from this region are listed in Table I. According to x-ray powder diffraction data little, if any (see Fig. 8), to a few vol. % of the orthorhombic $\text{ErSi}_x\text{Ge}_{1-x}$ impurity phase can be found in the as-prepared alloys from this phase region.

Considering magnetic properties of $\text{Er}_5\text{Si}_{3.5}\text{Ge}_{0.5}$ as an example representative for this phase region, both the dc magnetization and ac magnetic susceptibility measurements (Fig. 9) indicate antiferromagnetic (or ferrimagnetic) ordering at ~ 25 K. The paramagnetic Curie temperature of $\text{Er}_5\text{Si}_{3.5}\text{Ge}_{0.5}$ (Table II) is positive and the effective magnetic moment is nearly identical to that of the free Er^{3+} ion.

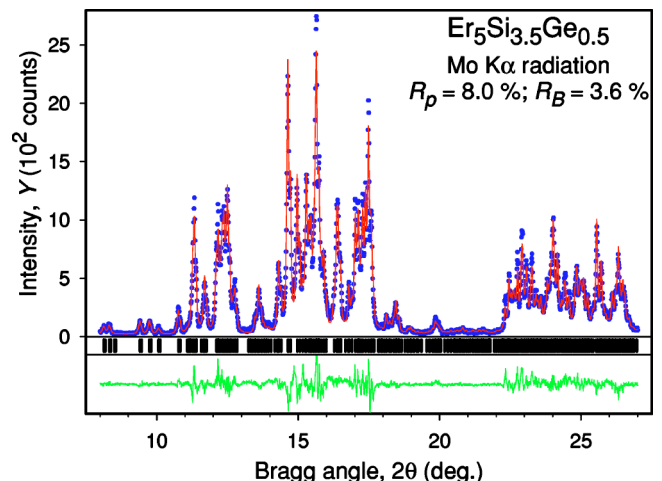


FIG. 8. (Color online) A fragment of the x-ray powder diffraction pattern of the $\text{Er}_5\text{Si}_{3.5}\text{Ge}_{0.5}$ alloy. The points represent observed data and the line drawn through the data points corresponds to the calculated pattern. The difference, $Y_{\text{obs}} - Y_{\text{calc}}$, is shown at the bottom of the plot. The set of vertical bars represents calculated positions of Bragg peaks (for both $K\alpha_1$ and $K\alpha_2$ components) of the monoclinic $\text{Er}_5\text{Si}_{3.5}\text{Ge}_{0.5}$.

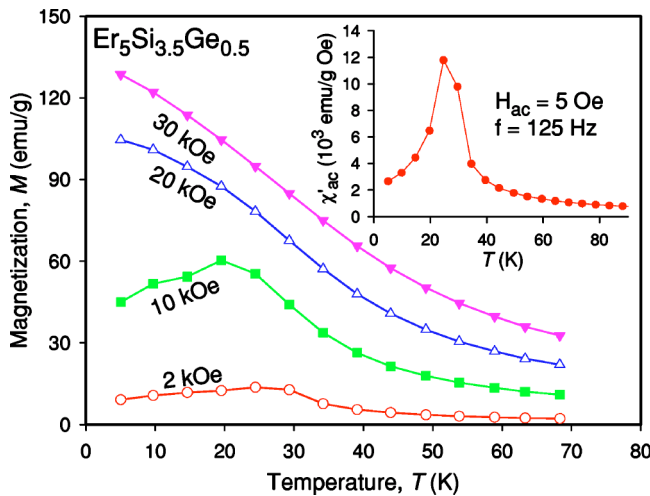


FIG. 9. (Color online) The dc magnetization of $\text{Er}_5\text{Si}_{3.5}\text{Ge}_{0.5}$ measured as a function of temperature in 2, 10, 20, and 30 kOe magnetic fields. The inset shows the behavior of the ac magnetic susceptibility of $\text{Er}_5\text{Si}_{3.5}\text{Ge}_{0.5}$.

The low temperature heat capacity measured in a zero magnetic field, which is shown in Fig. 10, displays a λ -type anomaly with a maximum at 28 K indicating that the magnetic ordering in $\text{Er}_5\text{Si}_{3.5}\text{Ge}_{0.5}$ is a second-order phase transformation. Additional weak heat capacity anomaly observed around 10 K in a zero magnetic field is consistent with the anomalous behavior of the magnetization at $T \approx 10$ K in 2 kOe and 10 kOe magnetic fields, see Fig. 9. Neither the heat capacity nor magnetic measurements indicate any other transitions between ~ 4 K and ~ 350 K. The λ -type anomaly is transformed into a cusp at ~ 22 K by a 10 kOe magnetic field, which also points to an antiferromagnetic ground state of the material. Magnetic fields exceeding 10 kOe, however, suppress the magnetic contribution to heat capacity below the zero magnetic field magnetic ordering temperature (T_N) but broaden and increase it immediately above the zero magnetic field T_N , which is typical of ferromagnetic behavior.

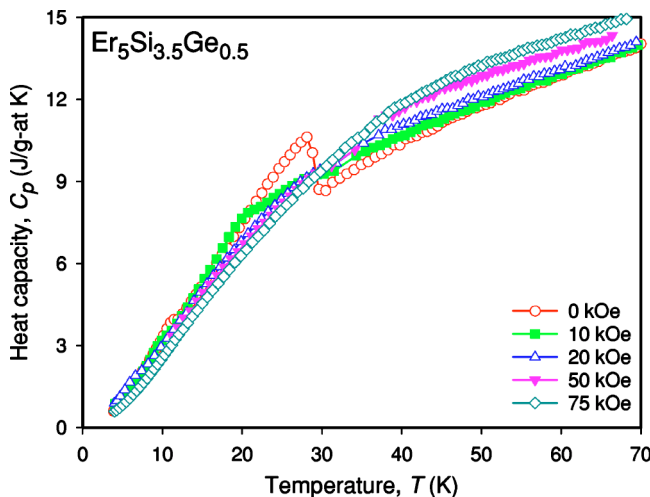


FIG. 10. (Color online) The low temperature heat capacity of $\text{Er}_5\text{Si}_{3.5}\text{Ge}_{0.5}$ measured in 0, 10, 20, 50, and 75 kOe magnetic fields after zero-field cooling the sample to ~ 3.5 K.

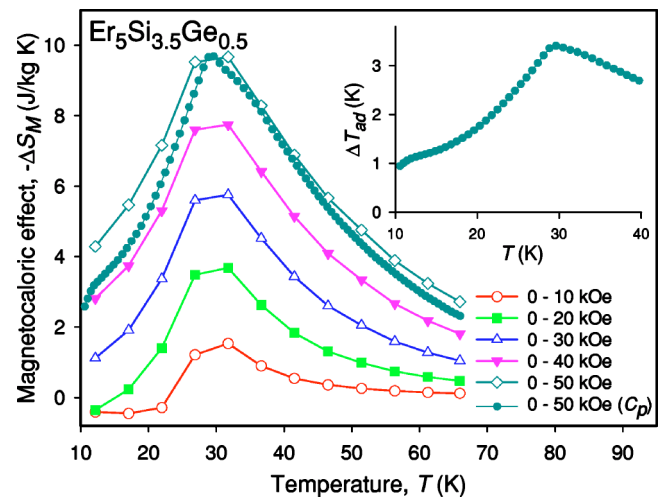


FIG. 11. (Color online) The isothermal magnetic entropy change in $\text{Er}_5\text{Si}_{3.5}\text{Ge}_{0.5}$ calculated from both heat capacity (solid circles) and magnetization (all other data points) measurements. The inset illustrates the adiabatic temperature change for 0 to 50 kOe magnetic field change calculated from heat capacity data.

These features are in agreement with the isothermal magnetization of $\text{Er}_5\text{Si}_{3.5}\text{Ge}_{0.5}$ measured at $T = 5$ K (Fig. 3), which shows a metamagnetic-like transformation with a critical magnetic field around 11 kOe.

The magnetic moment remains near 60% of its expected saturation value of $9\mu_B$ per Er atom in a 50 kOe magnetic field. Unlike in the pure Er_5Si_4 , a 75 kOe magnetic field does not induce an additional low temperature transformation(s) as can be concluded from the absence of any additional heat capacity peaks in $\text{Er}_5\text{Si}_{3.5}\text{Ge}_{0.5}$. It is feasible, however, that magnetostructural transitions may be induced in this phase region by magnetic fields greater than 75 kOe. The magnetocaloric effect of $\text{Er}_5\text{Si}_{3.5}\text{Ge}_{0.5}$ shown in Fig. 11 is moderate, and it is slightly smaller than that of Er_5Si_4 .

Erbium germanide: Er_5Ge_4 and the corresponding solid solution

Beginning from the $\text{Er}_5\text{Si}_3\text{Ge}$ stoichiometry and ending with the 5:4 erbium germanide, the as-prepared alloys crystallize in the Sm_5Ge_4 -type structure at room temperature, thus making it the most extensive solid solution region in the $\text{Er}_5\text{Si}_x\text{Ge}_{4-x}$ system. The alloy with the $\text{Er}_5\text{Si}_{3.2}\text{Ge}_{2.8}$ composition contains both the monoclinic $\text{Gd}_5\text{Si}_2\text{Ge}_2$ -type and the orthorhombic Sm_5Ge_4 -type phases, thus indicating that a narrow two-phase region separates the intermediate monoclinic phase and the Er_5Ge_4 -based solid solution in this system. Since the boiling temperature of Ge (2830°C) is considerably lower than that of Si (3145°C) and it is slightly lower than the boiling temperature of Er (2868°C), losses of Ge due to evaporation begin to exceed losses of Er during the arc melting, and a small amount (~ 5 vol. % according to Rietveld refinement) of Er_5Ge_3 phase forms in the as-prepared Er_5Ge_4 , see Fig. 12. The unit cell parameters of several alloys from this extended solid solution region are listed in Table I.

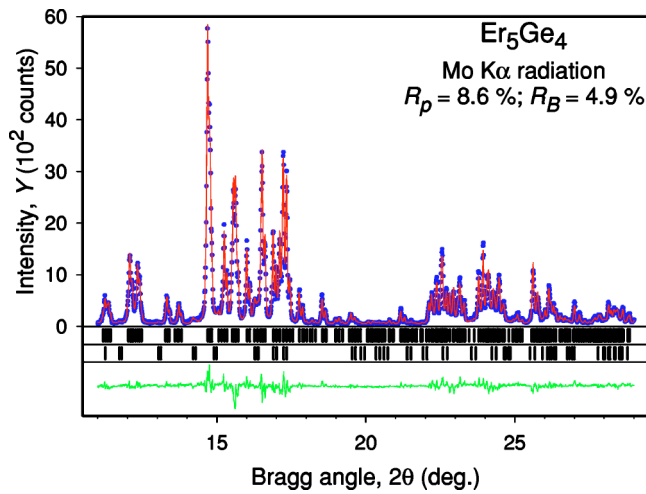


FIG. 12. (Color online) A fragment of the x-ray powder diffraction pattern of the Er_5Ge_4 alloy. The points represent observed data and the line drawn through the data points corresponds to the calculated pattern. The difference, $Y_{\text{obs}} - Y_{\text{calc}}$, is shown at the bottom of the plot. The upper set of vertical bars represents calculated positions of Bragg peaks (both $K\alpha_1$ and $K\alpha_2$ components) of the orthorhombic Er_5Ge_4 , and the lower set of vertical bars indicates the same for Er_5Ge_3 , which belongs to the hexagonal Mn_5Si_3 -type structure.

The dc magnetization measurements indicate that $\text{Er}_5\text{Si}_3\text{Ge}$ (Fig. 13), $\text{Er}_5\text{Si}_{2.5}\text{Ge}_{1.5}$, $\text{Er}_5\text{Si}_{1.95}\text{Ge}_{2.05}$, and Er_5Ge_4 (Fig. 13) order antiferromagnetically at ~ 20 , ~ 18 , ~ 17 , and ~ 14 K, respectively. The Curie-Weiss parameters of these three alloys are found in Table II. For Er_5Ge_4 , they are in fair agreement with those reported by Holtzberg *et al.*² The low temperature heat capacity of Er_5Ge_4 is shown in Fig. 14. The λ -type anomaly, observed in a zero magnetic field around 14 K, corresponds to the cusp observed at the same temperature in the low magnetic field dc magnetization data and it indicates that the transition is second order. Zero magnetic field heat capacity of Er_5Ge_4 also displays additional cusp-

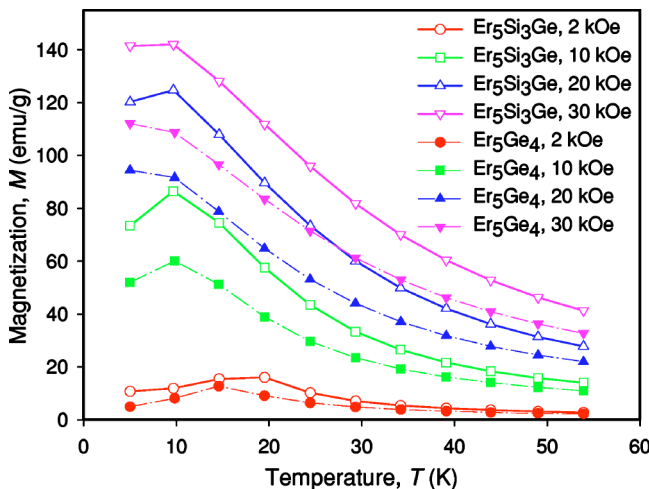


FIG. 13. (Color online) The dc magnetization of $\text{Er}_5\text{Si}_3\text{Ge}$ and Er_5Ge_4 measured as a function of temperature in 2, 10, 20, and 30 kOe magnetic fields.

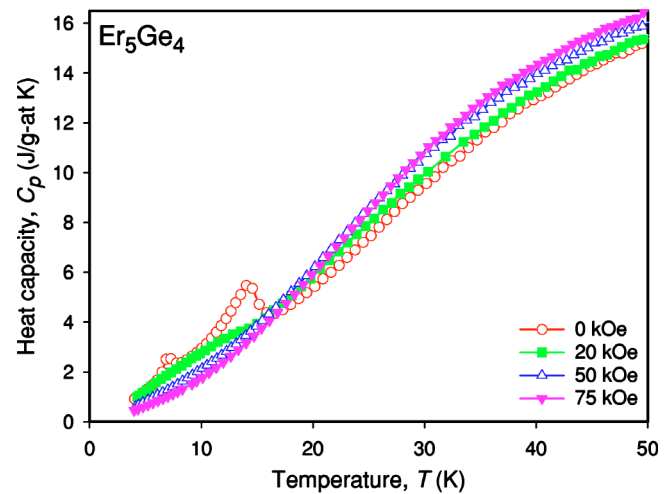


FIG. 14. (Color online) The low temperature heat capacity of Er_5Ge_4 measured in 0, 20, 50, and 75 kOe magnetic fields after zero-field cooling the sample to ~ 3.5 K.

like anomaly at ~ 7.5 K, which is not seen in the magnetization data, likely due to the lack of available experimental data points. Considering that the magnetic ordering temperature of the Er_5Ge_3 impurity is 38 K,⁴⁸ this heat capacity cusp seems to be intrinsic to Er_5Ge_4 , however, more detailed investigations are needed before its nature is better understood. Behavior of the heat capacity in nonzero magnetic fields is consistent with the isothermal magnetization of Er_5Ge_4 measured at $T=5$ K (Fig. 3), which shows a metamagneticlike transformation with a critical magnetic field around 6 kOe.

Similar to the other $\text{Er}_5\text{Si}_3\text{Ge}_{4-x}$ alloys, the magnetic moment of Er_5Ge_4 is about 60% of its expected saturation value of $9\mu_B$ per Er atom in a 50 kOe magnetic field. The magnetocaloric effect in the germanide (Fig. 15) is moderate and its maximum value is nearly the same as that of the 5:4 erbium silicide.

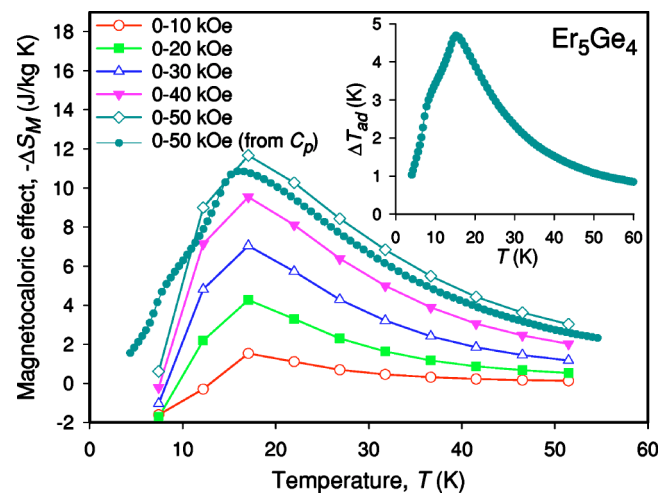


FIG. 15. (Color online) The isothermal magnetic entropy change in Er_5Ge_4 calculated from both heat capacity (solid points) and magnetization (all other data points) measurements. The inset illustrates the adiabatic temperature change for 0 to 50 kOe magnetic field change calculated from heat capacity data.

CONCLUSIONS

Although at present we do not have enough experimental data to propose even a preliminary composition-temperature diagram in order to summarize phase relationships and magnetism of the $\text{Er}_5\text{Si}_x\text{Ge}_{4-x}$ system, it is clear that the magnetic behaviors are more different than similar when compared with the $\text{Gd}_5\text{Si}_x\text{Ge}_{4-x}$ system. Both systems are analogous in that there are two structurally different orthorhombic phases (Er_5Si_4 and the Er_5Ge_4 -based solid solution vs the Gd_5Si_4 -based and Gd_5Ge_4 -based solid solutions) which are separated by the monoclinic phase region. Furthermore, substituting Si by Ge has similar effect on the room temperature crystallography in both systems: increasing the concentration of Ge results first, in the loss of one-half of the Si_2 dimers between the slabs (monoclinic phase) and second, all of the interslab Si_2 dimers in the Er_5Ge_4 -based and in the Gd_5Ge_4 -based solid solutions.

The most significant differences, in addition to the extent of the three phase regions in paramagnetic state, are as follows: first, the magnetic ordering temperatures of $\text{Er}_5\text{Si}_x\text{Ge}_{4-x}$ alloys are much lower than those of $\text{Gd}_5\text{Si}_x\text{Ge}_{4-x}$ alloys; second, the magnetic ordering temperatures show a weak dependence on the composition (i.e., on the value of x) in the Er-based system and the magnetic structures appear to be quite complex; third, in all the studied $\text{Er}_5\text{Si}_x\text{Ge}_{4-x}$ alloys, the magnetic ordering is decoupled from the crystal lattice in low magnetic fields; fourth, it appears that in magnetic fields lower than ~ 80 kOe, a magnetostructural transition is observed only in Er_5Si_4 ; and fifth, the magnetocaloric effect in the $\text{Er}_5\text{Si}_x\text{Ge}_{4-x}$ system is much lower than that in the

$\text{Gd}_5\text{Si}_x\text{Ge}_{4-x}$ system, where both the crystal and magnetic lattices are not only coupled but they are easily affected by relatively low magnetic fields over a broad range of concentrations.

An intriguing observation that magnetic fields as low as 40 kOe may affect the temperature of the crystallographic-only transformation from the paramagnetic monoclinic Er_5Si_4 to the orthorhombic Gd_5Si_4 -type polymorph, which is also paramagnetic, is likely related to large localized magnetic moments of Er and to unusually strong spin-orbit coupling. Its understanding requires further experimental and theoretical studies. It is also important to emphasize that many of the as arc-melted $\text{Er}_5\text{Si}_x\text{Ge}_{4-x}$ alloys can contain small amounts of impurity $\text{ErSi}_x\text{Ge}_{1-x}$ or $\text{Er}_5\text{Si}_x\text{Ge}_{3-x}$ phases, which may somewhat affect both the observed behavior and the interpretation of the data.

Note added in proof. As follows from recent quantitative x-ray powder diffraction analysis,⁴⁹ only ~ 40 mol.% of the monoclinic Er_5Si_4 is converted into the orthorhombic Er_5Si_4 phase during slow heating between 190 and 240 K. The entropy of the corresponding polymorphic transformation, therefore, should be increased from the mentioned above 0.24 J/g at K to ~ 0.6 J/g at K.

ACKNOWLEDGMENTS

The authors thank D. C. Kesse and J. L. Anderson for their help in preparing some of the $\text{Er}_5\text{Si}_{4-x}\text{Ge}_x$ alloys. This work was supported by the Office of Basic Energy Sciences, Materials Sciences Division of the U.S. Department of Energy under Contract No. W-7405-ENG-82.

*Electronic address: vitkp@ameslab.gov

¹G. S. Smith, A. G. Tharp, and Q. Johnson, *Nature (London)* **210**, 1148 (1966); **210**, 1148 (1966).

²F. Holtzberg, R. J. Gambino, and T. R. McGuire, *J. Phys. Chem. Solids* **28**, 2283 (1967).

³E. M. Levin, V. K. Pecharsky, K. A. Gschneidner, Jr., and G. J. Miller, *Phys. Rev. B* **64**, 235103 (2001).

⁴E. M. Levin, K. A. Gschneidner, Jr., and V. K. Pecharsky, *Phys. Rev. B* **65**, 214427 (2002).

⁵C. Magen, L. Morellon, P. A. Algarabel, C. Marquina, and M. R. Ibarra, *J. Phys.: Condens. Matter* **15**, 2389 (2003).

⁶V. K. Pecharsky, A. P. Holm, K. A. Gschneidner, Jr., and R. Rink, *Phys. Rev. Lett.* **91**, 197204 (2003).

⁷C. Magen, Z. Arnold, L. Morellon, Y. Skorokhod, P. A. Algarabel, M. R. Ibarra, and J. Kamarad, *Phys. Rev. Lett.* **91**, 207202 (2003).

⁸H. Tang, V. K. Pecharsky, K. A. Gschneidner, Jr., and A. O. Pecharsky, *Phys. Rev. B* **69**, 064410 (1994).

⁹E. M. Levin, K. A. Gschneidner, Jr., T. A. Lograsso, D. L. Schlagel, and V. K. Pecharsky, *Phys. Rev. B* **69**, 144428 (2004).

¹⁰V. K. Pecharsky and K. A. Gschneidner, Jr., *Phys. Rev. Lett.* **78**, 4494 (1997).

¹¹V. K. Pecharsky and K. A. Gschneidner, Jr., *J. Alloys Compd.* **260**, 98 (1997).

¹²L. Morellon, J. Blasco, P. A. Algarabel, and M. R. Ibarra, *Phys. Rev. B* **62**, 1022 (2000).

¹³A. O. Pecharsky, K. A. Gschneidner, Jr., V. K. Pecharsky, and C. E. Schindler, *J. Alloys Compd.* **338**, 135 (2002).

¹⁴V. K. Pecharsky and K. A. Gschneidner, Jr., *Appl. Phys. Lett.* **70**, 3299 (1997).

¹⁵L. Morellon, C. Magen, P. A. Algarabel, M. R. Ibarra, and C. Ritter, *Appl. Phys. Lett.* **79**, 1318 (2001).

¹⁶L. Morellon, C. Ritter, C. Magen, P. A. Algarabel, and M. R. Ibarra, *Phys. Rev. B* **68**, 024417 (2003).

¹⁷H. Huang, A. O. Pecharsky, V. K. Pecharsky, and K. A. Gschneidner, Jr., *Adv. Cryog. Eng.* **48**, 11 (2002).

¹⁸C. Ritter, L. Morellon, P. A. Algarabel, C. Magen, and M. R. Ibarra, *Phys. Rev. B* **65**, 094405 (2002).

¹⁹O. Tegus, O. Dagula, E. Brück, L. Zhang, F. R. deBoer, and K. H. J. Buschow, *J. Appl. Phys.* **91**, 8534 (2002).

²⁰N. P. Thuy, N. V. Nong, N. T. Hien, L. T. Tai, T. Q. Vinh, P. D. Thang, and E. Brück, *J. Magn. Magn. Mater.* **242–245**, 841 (2002).

²¹N. P. Thuy, *Solid State Technol.* **10**, 1 (2002).

²²Y. D. Yoa, S. F. Lee, M. D. Lee, K. D. Wu, D. G. Chen, N. P. Thuy, N. T. Hien, L. T. Tai, T. D. Vinh, and N. V. Nong, *Physica B* **327**, 324 (2003).

²³S. J. Lee, J. M. Park, J. E. Snyder, D. C. Jiles, D. L. Schlagel, T.

- A. Lograsso, A. O. Pecharsky, and D. W. Lynch, *Appl. Phys. Lett.* **84**, 1865 (2004).
- ²⁴K. A. Gschneidner, Jr., V. K. Pecharsky, A. O. Pecharsky, V. V. Itchenko, and E. M. Levin, *J. Alloys Compd.* **303–304**, 214 (2000).
- ²⁵V. V. Itchenko, V. K. Pecharsky, and K. A. Gschneidner, Jr., *Adv. Cryog. Eng.* **46A**, 405 (2000).
- ²⁶N. P. Thuy, Y. Y. Chen, Y. D. Yao, C. R. Wang, S. H. Lin, J. C. Ho, T. P. Nguyen, P. D. Thang, J. C. P. Klaasse, N. T. Hien, and L. T. Tai, *J. Magn. Magn. Mater.* **262**, 432 (2003).
- ²⁷R. Cerny and K. Alami-Yadri, *Acta Cryst.* **E59**, i1 (2003).
- ²⁸M. Pani and A. Palenzona, *J. Alloys Compd.* **360**, 151 (2003).
- ²⁹S. P. Luzan, V. E. Listovnichii, Yu. I. Buyanov, and P. S. Martsenyuk, *J. Alloys Compd.* **239**, 77 (1996).
- ³⁰B. Y. Kotur and O. V. Parasyuk, *Russ. Metall.* **1994**, 134 (1994).
- ³¹V. K. Pecharsky, A. O. Pecharsky, Y. Mozharivskiy, K. A. Gschneidner, Jr., and G. J. Miller, *Phys. Rev. Lett.* **91**, 207205 (2003).
- ³²Y. Mozharivskiy, A. O. Pecharsky, V. K. Pecharsky, G. J. Miller, and K. A. Gschneidner, Jr., *Phys. Rev. B* **69**, 144102 (2004).
- ³³A. P. Holm, V. K. Pecharsky, and K. A. Gschneidner, Jr. (unpublished).
- ³⁴B. A. Hunter, Rietica—a visual Rietveld program, IUCr Commission on Powder Diffraction Newsletter, N 20, Summer (1998) <http://www.rietica.org>
- ³⁵V. K. Pecharsky, J. O. Moorman, and K. A. Gschneidner, Jr., *Rev. Sci. Instrum.* **68**, 4196 (1997).
- ³⁶V. K. Pecharsky and K. A. Gschneidner, Jr., *J. Appl. Phys.* **86**, 565 (1999).
- ³⁷V. K. Pecharsky and K. A. Gschneidner, Jr., *J. Appl. Phys.* **86**, 6315 (1999).
- ³⁸V. K. Pecharsky and K. A. Gschneidner, Jr., *Adv. Mater. (Weinheim, Ger.)* **13**, 683 (2001).
- ³⁹W. Choe, V. K. Pecharsky, A. O. Pecharsky, K. A. Gschneidner, Jr., V. G. Young, Jr., and G. J. Miller, *Phys. Rev. Lett.* **84**, 4617 (2000).
- ⁴⁰P. Thuéry, G. André, F. El Maziani, M. Clin, and P. Schobinger-Papamentellos, *J. Magn. Magn. Mater.* **109**, 197 (1992).
- ⁴¹N. Van Nhung, J. Sivadriere, and A. Apostolov, *Colloq. Int. C. N. R. S.* **180**, 261 (1970).
- ⁴²J. M. Cadogan, D. H. Ryan, Z. Altounian, X. Liu, and I. P. Swainson, *J. Appl. Phys.* **95**, 7076 (2004).
- ⁴³K. A. Gschneidner, Jr., *J. Alloys Compd.* **193**, 1 (1993).
- ⁴⁴When our work was completed and undergoing a review, Cadogan *et al.* (Ref. 42) reported a neutron scattering study of Er_5Si_4 . Their Er_5Si_4 specimen does not exhibit a structural transition from the high temperature orthorhombic Gd_5Si_4 -type structure to the low temperature monoclinic $\text{Gd}_5\text{Si}_2\text{Ge}_2$ -type structure around 200 K found in our sample. The Er_5Si_4 alloy of Ref. 42 retains the Gd_5Si_4 -type structure between 4 K and 300 K, which is likely a consequence of employing commercial “99.9%” purity Er in the sample preparation. Although the results of Ref. 42 are most certainly affected by the high concentration of interstitial impurities that are normally present in commercial-purity Er (see Ref. 43), the magnetic structure of impurities-stabilized orthorhombic $\text{Er}_5\text{Si}_4(\text{C}_x\text{O}_y \cdots)$ is complex and temperature dependent, which is consistent with the magnetic properties of the monoclinic Er_5Si_4 samples employed in this study.
- ⁴⁵The sample used in the magnetization measurements shown in Fig. 4 was a piece collected after a large grain located in sample III was used to cut a single crystal from the Er_5Si_4 specimen. Neither the single crystalline nature, nor the orientation of this piece was analyzed using a backscatter Laue technique. It is, therefore, possible that the sample contained several small grains with similar orientations.
- ⁴⁶V. K. Pecharsky, G. D. Samolyuk, V. P. Antropov, A. O. Pecharsky, and K. A. Gschneidner, Jr., *J. Solid State Chem.* **171**, 57 (2003).
- ⁴⁷V. K. Pecharsky and K. A. Gschneidner, Jr. (unpublished).
- ⁴⁸A. P. Vokhmyanin and Yu. A. Dorofeev, *Phys. Solid State* **45**, 1735 (2003).
- ⁴⁹Ya. Mudryk, V. K. Pecharsky, and K. A. Gschneidner, Jr. (unpublished).